

Calculation of Jupiter's Size, Saturn's Size, Tides and Zonal Winds by Quantum Gravity Theory

Huaiyang Cui

Department of Physics, Beihang University, Beijing, 102206, China

Email: hycui@buaa.edu.cn

(October 30, 2023 version 1, January 5, 2024 version 2, submitted to viXra)

Abstract: In recent years, de Broglie matter wave has been generalized in terms of the ultimate acceleration on planetary-scale. This paper shows that the Jupiter's size and Saturn's size are the consequence of the interference of the generalized matter waves on planetary-scale. In this calculation, Jupiter's radius is determined as $7.1491e+7m$ with a relative error of 5.05%; Saturn's radius is determined as $5.80057e+7m$ with a relative error of 3.75%. This calculation also correctly predicts the locations of Halo ring and main ring for the Jupiter; ring A, B, C and D for the Saturn. In this calculation to the Earth, the tide near the equator has one maximal peak and 45 billows on the circumference around the Earth; the tide occurs every 24.91 hours, the width of the maximal peak of the tide is 1741km which lasts about 1.04 hours. At the latitude $35.4^\circ N$, its tide has two maximal peaks and 68 billows on its circumference around the Earth at the latitude, where the tide occurs every 12.45 hours. The equatorial belt has an eastward sea-flow at the speed of about 1m/s; on the north hemisphere, between latitudes $0.1^\circ N$ and $35.4^\circ N$ there is a larger ocean circulation; between latitudes $35.4^\circ N$ and $90^\circ N$ there is another ocean circulation. This paper shows that the Jupiter's south hemisphere contains five belts/zones that are separated by five coherent ridges at $0^\circ S$, $28^\circ S$, $41.6^\circ S$, $54.5^\circ S$ and $70^\circ S$, respectively, with the maximal wind of 120m/s, the Great Red Spot lives constantly at $23^\circ S$. the Saturn's south hemisphere contains six belts/zones that are separated by six coherent ridges, with the maximal wind of 420m/s. These predictions agree well with the experimental observations.

1. Introduction

The concept of generalized relativistic matter wave and its applications were proposed and investigated in the author's early paper [1], the present paper continues to discuss the generalized relativistic matter wave and its extensions to the geophysics and planetary science [2,3,4].

In analogy with the ultimate speed c , there is an ultimate acceleration β , nobody's acceleration can exceed this limit β in a many-body system. In recent years, de Broglie matter wave [5,6,7] has been generalized in terms of the ultimate acceleration. Consider a particle, its generalized relativistic matter wave is given by the path integral

$$\psi = \exp\left(\frac{i\beta}{c^3} \int_0^x (u_1 dx_1 + u_2 dx_2 + u_3 dx_3 + u_4 dx_4)\right) . \quad (1)$$

where u is the 4-velocity of the particle, β is the ultimate acceleration determined by experiments. The β has replaced the *Planck constant* in this quantum gravity theory so that *its wavelength becomes a length on planetary-scale*. The early paper [1] shows that stellar size and planetary size are the consequence of the interference of the generalized matter waves,

thus by this way, the solar radius is determined as $7e+8$ (m) with a relative error of 0.72%; the Earth's radius is determined as $6.4328e+6$ (m) with a relative error of 0.86%.

The present paper shows that this quantum gravity theory with the ultimate acceleration provides a mechanism which allows us to calculate the Jupiter's size and Saturn's size, to calculate the tidal periods and ocean circulations on the Earth's surface, to calculate the zonal winds and spots on Jupiter and Saturn.

2. Extracting the ultimate acceleration from a system

Similar to the Bohr model of hydrogen atom, the orbital circumference is n multiple of the wavelength of the planetary-scale relativistic matter wave. According to Eq. (1), consider a satellite, we have

$$\left. \begin{aligned} \frac{\beta}{c^3} \oint_L v_l dl = 2\pi n \\ v_l = \sqrt{\frac{GM}{r}} \end{aligned} \right\} \Rightarrow \sqrt{r} = \frac{c^3}{\beta\sqrt{GM}} n; \quad n = 0, 1, 2, \dots \quad (2)$$

This orbital quantization rule only achieves a half success on the Jupiter system and Saturn system, as shown in Figure 1. The Jupiter, Metis, Adrastea, Amalthea and Thebe satisfy the quantization equation in Figure 1(a); while other outer satellites (Io, Europa, Ganymede, Callisto) fail. The Saturn, Mimas, Enceladus, Tethys and Dione satisfy the quantization equation in Figure 1(b); while other outer satellites (Rhea, Titan, Hyperion, Iapetus) fail. But, since we only study quantum gravity effects near the planets, so this orbital quantization rule is good enough as a foundational quantum theory. In Figure 1, the blue straight lines express a linear regression relation among the quantized orbits, so it gives Jupiter's $\beta=4.013970e+10$ (m/s^2) and Saturn's $\beta=7.175115e+13$ (m/s^2) by fitting the lines. The quantum numbers $n=6, 7, 8, \dots$ were assigned to the Jupiter's satellites, the Jupiter was assigned a quantum number $n=0$ because it is in the **central state**. The quantum numbers $n=7, 8, 9, \dots$ were assigned to the Saturn's satellites, the Saturn was assigned a quantum number $n=0$ because it is in the **central state**.

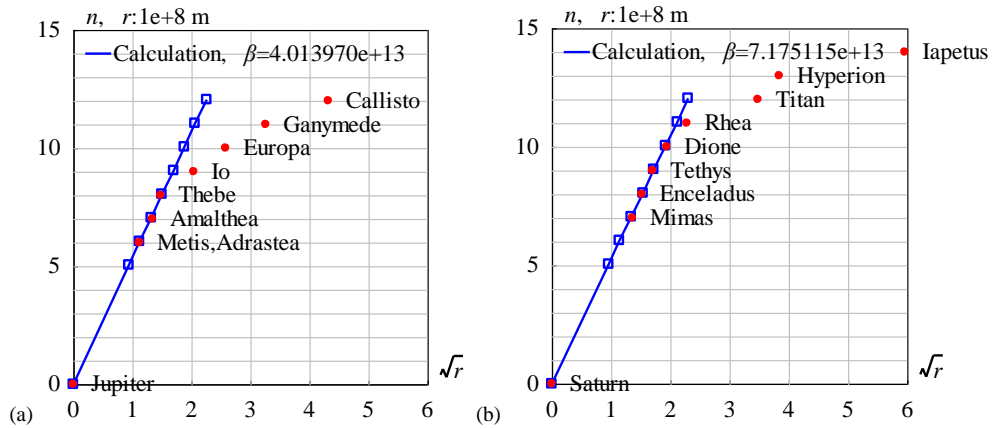


Figure 1 The inner satellites are quantized.

<Clet2020 Script>// C source code [8]
int i,j,k,n,N,N1,nP[10],Figure; double x,y,z,r,r1,rs,M,r_unit,H,beta,pD[10],D[200],S[200];
double orbit[20]={0,1.285,1.29,1.81,2.22,4.21,6.71,10.7,18.82,},a,b,A,B,r_massive,R;

```

double e[20]={0,0.0077,0.0063,0.0075,0.0180,0.0041,0.0094,0.0011,0.0074,0,0,0,};
int qn[20]={0,6,6,7,8,9,10,11,12,13,14,15,16,17,18,19,20}; char str[200];
char Stars[100]={"Jupiter; ;Metis,Adrastea;Amalthea;Thebe;Io;Europa;Ganymede;Callisto;"};
main(){ Figure=1; N=9;N1=5;rs=11.209*6.378e6;M=317.8*5.97237E24;r_unit=1e8;
for(i=0;i<N;i+=1) {y=e[i]; x=orbit[i]*(1+sqrt(1-y*y))/2; D[i]=sqrt(x); D[i+1]=qn[i]; }
nP[0]=REGRESSION; nP[1]=N1; DataJob(nP,D,pD); a=pD[0]; b=pD[1];
beta=b*SPEEDC*SPEEDC*SPEEDC/sqrt(GRAVITYC*M*r_unit); S[0]=0;S[1]=0;
SetAxis(X_AXIS,0,0,6,"#if#rs#t;0;1;2;3;4;5;6;");
SetAxis(Y_AXIS,0,0,15,"#ifn, r#t:1e+8 m;0;5;10;15;");
DrawFrame(0x016f,1,0xaffaf); A=-0.55; r_massive=2.7; R=sqrt(r_massive); B=-0.05;
rs/=r_unit;k=1; n=1; N1=10000;
for(i=0;i<N1;i+=1) { r=35*i/N1; r1=sqrt(r); y=a+b*r1;
if(Figure==2 && r1>R) y+=A*b*(r1-R)+B*b*R*r/r_massive;
if(y>=n) {S[k+k]=r1; S[k+k+1]=y; n+=1; if(r>rs) k+=1; } if(y>12) break;}
Format(str,"Calculation, #if#t=#e",beta); SetPen(2,0x0000ff);
Polyline(k,S,0,2,14,str);Plot("CARD,0,@k,XY,4,4,"S);
SetPen(2,0xff0000); Plot("OVALFILL,0,@N,XY,3,3,"D); nP[0]=TAKE;
for(i=0;i<N;i+=1) { nP[1]=i;TextJob(nP,Stars,str); TextHang(D[i+1]+0.3,D[i+1],0,str);}
}#v07=?>A#t

```

```

<Clet2020 Script>// C source code [8]
int i,j,k,n,N,N1,nP[10],Figure; double x,y,z,r,r1,rs,M,r_unit,H,beta,pD[10],D[200],S[200];
double orbit[20]={0,1.85,2.37,2.94,3.77,5.27,12.21,14.8,35.6,},a,b,A,B,r_massive,R;
double e[20]={0,0,0,0,0,0,0,0,0,0,0,}; int qn[20]={0,7,8,9,10,11,12,13,14,15,16,17,18,19,20};
char Stars[100]={"Saturn;Mimas;Enceladus;Tethys;Dione;Rhea;Titan;Hyperion;Iapetus;"}; char str[200];
main(){ Figure=1; N=9;N1=5; rs=9.449*6.378e6;M=95.16*5.97237E24;r_unit=1E8;
for(i=0;i<N;i+=1) {y=e[i]; x=orbit[i]*(1+sqrt(1-y*y))/2; D[i]=sqrt(x); D[i+1]=qn[i]; }
nP[0]=REGRESSION; nP[1]=N1; DataJob(nP,D,pD); a=pD[0]; b=pD[1];
beta=b*SPEEDC*SPEEDC*SPEEDC/sqrt(GRAVITYC*M*r_unit); S[0]=0; S[1]=0;
SetAxis(X_AXIS,0,0,6,"#if#rs#t;0;1;2;3;4;5;6;");
SetAxis(Y_AXIS,0,0,15,"#ifn, r#t:1e+8 m;0;5;10;15;");
DrawFrame(0x016f,1,0xaffaf); A=-0.62; r_massive=4.5; R=sqrt(r_massive); B=-0.05;
k=1; n=1; N1=10000; rs/=r_unit;
for(i=0;i<N1;i+=1) { r=40*i/N1; r1=sqrt(r); y=a+b*r1;
if(Figure==2 && r1>R) y+=A*b*(r1-R)+B*b*R*r/r_massive;
if(y>=n) {S[k+k]=r1; S[k+k+1]=y; n+=1; if(r>rs) k+=1; } if(y>12) break;}
Format(str,"Calculation, #if#t=#e",beta); SetPen(2,0x0000ff);
Polyline(k,S,0,2,14,str);Plot("CARD,0,@k,XY,4,4,"S);
SetPen(2,0xff0000); Plot("OVALFILL,0,@N,XY,3,3,"D); nP[0]=TAKE;
for(i=0;i<N;i+=1) { nP[1]=i;TextJob(nP,Stars,str); TextHang(D[i+1]+0.3,D[i+1],0,str);}
}#v07=?>A#t

```

The relativistic matter wave function ψ needs a further explanation. In quantum mechanics, $|\psi|^2$ equals to the probability of finding an electron due to Max Born's explanation; in astrophysics, $|\psi|^2$ equals to the probability of finding a nucleon (proton or neutron) *averagely on an astronomic scale*, we have

$$|\psi|^2 \propto \text{nucleon-density} \propto \rho . \quad (3)$$

3. Jupiter's size and Saturn's size

In interior of Jupiter or Saturn, if the coherent length of the relativistic matter wave is long enough, its head may overlap with its tail when the particle moves in a closed orbit, as shown in Figure 2. Consider a point on the equatorial plane, the overlapped wave is given by

$$\begin{aligned}
\psi &= \psi(r)T(t) \\
\psi(r) &= \psi_0(1 + a_1 e^{i\delta} + a_2 e^{i2\delta} + \dots + a_{N-1} e^{i(N-1)\delta}) \\
\delta(r) &= \frac{\beta}{c^3} \oint_L (v_l) dl = \frac{2\pi\beta\omega r^2}{c^3}
\end{aligned} \quad (4)$$

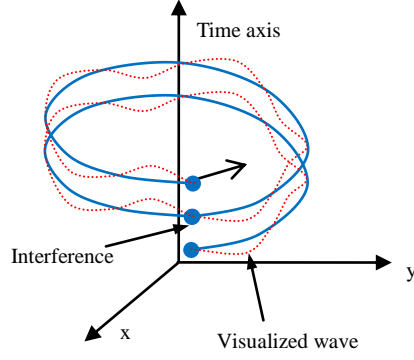


Figure 2 The head of the relativistic matter wave may overlap with its tail.

where N is the overlapping number which is determined by the coherent length of the relativistic matter wave, δ is the phase difference after one orbital motion, ω is the angular speed of the Jupiter rotation, a_1, a_2, \dots, a_{N-1} are the amplitudes of the wavelets. The above equation is a multi-slit interference formula in optics.

According to the study of tropic cyclones on the Pacific ocean [1][17] where clouds have the overlapping number $N=2$, the Jupiter and Saturn also have $N=2$ because they are gaseous planets, thus

$$\psi(r) = \psi_0(1 + a_1 e^{i\delta}) = \psi_0[(1 + a_1 \cos \delta) + i a_1 \sin \delta] \quad (5)$$

Let r_s denotes the radius of planet, due to the skin effect into planetary interior, the amplitude of the first wavelet is simply assumed as

$$a_1 = \begin{cases} \left(\frac{r}{r_s}\right)^5 & r \leq r_s \\ 1 & r > r_s \end{cases} \quad (6)$$

then the Jupiter's size and Saturn's size can be estimated.

Jupiter's angular speed at its equator is known as $\omega=2\pi/(9.925 \times 3600)$ (s^{-1}). Its mass $317.816M_{\text{earth}}$, the well-known radius $11.209r_{\text{earth}}$, the mean density 1330 (kg/m^3), the constant $\beta=4.013970 \times 10^{10}$ (m/s^2). According to the $N=2$, the matter distribution of the $|\psi|^2$ is calculated in Figure 3(a), it agrees well with the general description of Jupiter interior. The radius of Jupiter is determined as $r_c=7.1491 \times 10^7$ (m) with a relative error of 5.05% in Figure 3(a), which indicates that the Jupiter radius strongly depends on its rotation.

Saturn's angular speed at its equator is known as $\omega=2\pi/(10.6562 \times 3600)$ (s^{-1}). Its mass $95.16M_{\text{earth}}$, the well-known radius $9.449r_{\text{earth}}$, the mean density 700 (kg/m^3), the constant $\beta=7.175115 \times 10^{13}$ (m/s^2). According to the $N=2$, the matter distribution of the $|\psi|^2$ is calculated in Figure 3(b), it agrees well with the general description of Saturn interior. The radius of Saturn is determined as $r_c=5.80057 \times 10^7$ (m) with a relative error of -3.75% in Figure 3(b), which indicates that the Saturn radius strongly depends on its rotation.

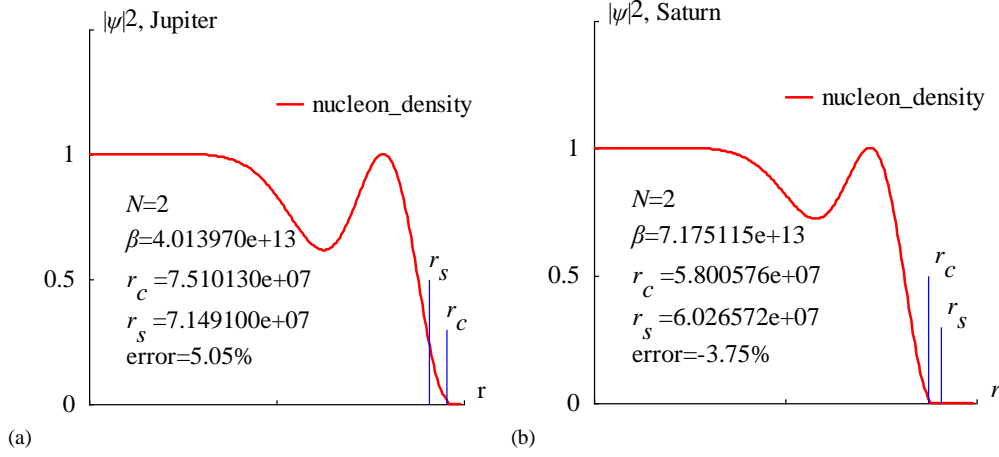


Figure 3 The nucleon distribution $|\psi|^2$ in radial direction is calculated. (a) Jupiter, (b) Saturn.

```
<Clet2020 Script>//C source code [8]
int i,j,k,n,N; double H,M,r,r_atm,r_unit,x,y,z,delta,D[10],S[1000];
double rs,rc,omega,amp,d,beta; char str[100];
main(){k=200;rs=11.209*6.378e6; r_atm =rs+rs/10; rc=r_atm; n=0; N=2;
beta=4.013970e+13;H=SPEEDC*SPEEDC*SPEEDC/beta; M=317.816*5.97237e24;
r_unit=r_atm/k; omega=2*PI/(9.925*60*60);//angular speed
for(i=0;i<k;i+=1) {r=i*r_unit; x=r/rs; amp=pow(x,5); d=(1+amp)*(1+amp); //skin effect
delta=2*PI*omega*r/H; x=1+amp*cos(delta);y=amp*sin(delta); z=(x*x+y*y)/d; if(r>rc) z=0;
S[n]=i;S[n+1]=z; n+=2; if(rc>=r_atm && z<0.02) rc=r; }
SetAxis(X_AXIS,0,0,k,"r; ; ;");SetAxis(Y_AXIS,0,0,1.5,"#if|ψ|²#su2#t, Jupiter;0;0.5;1; ;");
DrawFrame(FRAME_SCALE,1,0,axffaf); x=50;z=100*(rc-rs)/rs;
SetPen(2,0xff0000);Polyline(k,S,k/2,1.2," nucleon_density");SetPen(1,0xff);
x=rs/r_unit;y=0.5;D[0]=x;D[1]=0;D[2]=x;D[3]=y; Polyline(2,D);TextHang(x,y+0.1,0,"#ifr#sds#t");
x=rc/r_unit;y=0.3;D[0]=x;D[1]=0;D[2]=x;D[3]=y; Polyline(2,D);TextHang(x,y+0.1,0,"#ifr#sdc#t");
Format(str,"#ifN#t=#d#n#ifβ#t=#e#n#ifr#sdc#t =%e#n#ifr#sds#t =%e#nerror=%.2f% ".N,beta,rc,rs,z);
TextHang(k/10,0.8,0,str);
}#v07=?>A
```

```
<Clet2020 Script>//C source code [8]
int i,j,k,n,N; double H,M,r,r_atm,r_unit,x,y,z,delta,D[10],S[1000];
double rs,rc,omega,amp,d,beta; char str[100];
main(){k=200;rs=9.449*6.378e6; r_atm =rs+rs/10; rc=r_atm; n=0; N=2;
beta=7.175115e+13;H=SPEEDC*SPEEDC*SPEEDC/beta; M=95.16*5.97237e24;
r_unit=r_atm/k; omega=2*PI/(10.6562*60*60);//angular speed
for(i=0;i<k;i+=1) {r=i*r_unit; x=r/rs; amp=pow(x,5); d=(1+amp)*(1+amp); //skin effect
delta=2*PI*omega*r/H; x=1+amp*cos(delta);y=amp*sin(delta); z=(x*x+y*y)/d; if(r>rc) z=0;
S[n]=i;S[n+1]=z; n+=2; if(rc>=r_atm && z<0.02) rc=r; }
SetAxis(X_AXIS,0,0,k,"#ifr#t; ; ;");SetAxis(Y_AXIS,0,0,1.5,"#if|ψ|²#su2#t, Saturn;0;0.5;1; ;");
DrawFrame(FRAME_SCALE,1,0,axffaf); x=50;z=100*(rc-rs)/rs;
SetPen(2,0xff0000);Polyline(k,S,k/2,1.2," nucleon_density");SetPen(1,0xff);
x=rs/r_unit;y=0.3;D[0]=x;D[1]=0;D[2]=x;D[3]=y; Polyline(2,D);TextHang(x,y+0.1,0," #ifr#sds#t");
x=rc/r_unit;y=0.5;D[0]=x;D[1]=0;D[2]=x;D[3]=y; Polyline(2,D);TextHang(x,y+0.1,0," #ifr#sdc#t");
Format(str,"#ifN#t=#d#n#ifβ#t=#e#n#ifr#sdc#t =%e#n#ifr#sds#t =%e#nerror=%.2f% ".N,beta,rc,rs,z);
TextHang(k/10,0.8,0,str);
}#v07=?>A
```

4. Locations of satellites and rings

The calculation of near field situations has also been carried out by the same formula Eq.(4) as shown in Figure 4. For Jupiter, the maxima of $|\psi(r)|^2$ point out the orbital radii of Metis, Adrastea, Amalthea and Thebe, respectively; also approximately gives out the locations of Halo ring and Main ring; the overall relative error is about 5%.

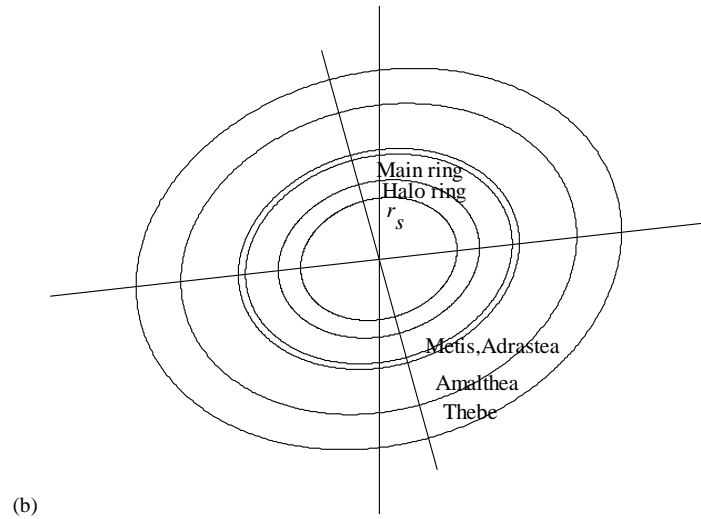
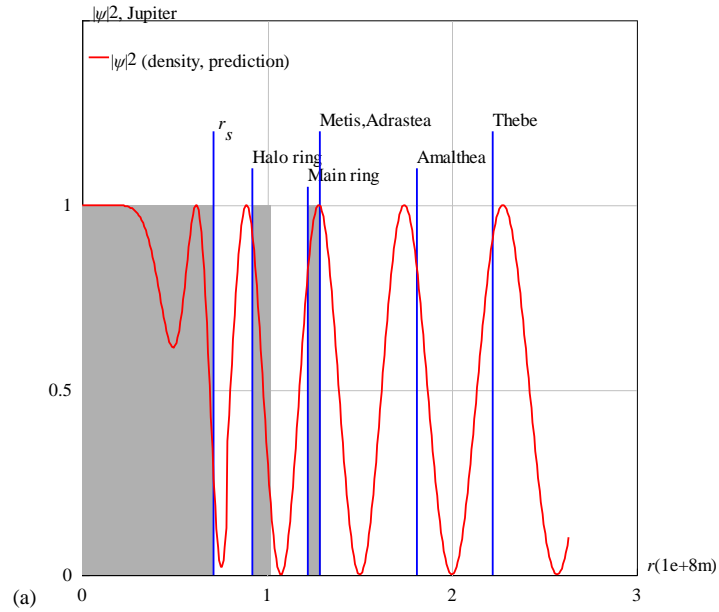


Figure 4 (a) The nucleon distribution $|\psi|^2$ is calculated in the radial direction for Jupiter. (b) Orbits

```
<Clet2020 Script>//C source code [8]
int i,j,k,n,N; double H,M,r,r_atm,r_unit,x,y,z,delta,D[10],S[1000];
double rs,rc,omega,amp,d,beta; char str[100];
main(){k=400;rs=11.209*6.378e6; r_atm =rs+rs/10; rc=r_atm; n=0; N=2;
beta=4.013970e+13;H=SPEEDC*SPEEDC*SPEEDC/beta; M=317.816*5.97237e24;
r_unit=3e+8/k; omega=2*PI/(9.925*60*60);//angular speed
for(i=0;i<k;i+=1) {r=i*r_unit; x=r/rs;
if(r<r_atm) {delta=2*PI*omega*r*r/H; amp=pow(x,5);}
else {delta=2*PI*sqrt(GRAVITYC*M*r)/H; amp=1;}
d=(1+amp)*(1+amp); x=1+amp*cos(delta); y=amp*sin(delta); z=(x*x+y*y)/d;
S[n]=i;S[n+1]=z; n+=2; if(i>350) break;}
SetAxis(X_AXIS,0,0,k,"#ifr#t(1e+8m);0;1;2;3;");SetAxis(Y_AXIS,0,0,1.5,"#if|ψ|²#t Jupiter;0;0.5;1;");
DrawFrame(0x0133,2,0xaffaf); SetPen(2,0xff);
x=rs/r_unit;y=1.2;D[0]=0;D[1]=0;D[2]=x;D[3]=1;
Draw("RECT,3,XY,0,0xb0b0b0",D);D[0]=D[2]; D[3]=y; Polyline(2,D);TextHang(x,y+0.03,0," #ifr#sds#t ");
x=0.92e8/r_unit;y=1.1;D[0]=x;D[1]=0;D[2]=1.02e8/r_unit;D[3]=1;
Draw("RECT,3,XY,0,0xb0b0b0",D); D[2]= D[0]; D[3]=y; Polyline(2,D);TextHang(x,y+0.03,0,"Halo ring");
x=1.22e8/r_unit;y=1.05;D[0]=x;D[1]=0;D[2]=1.29e8/r_unit;D[3]=1;
Draw("RECT,3,XY,0,0xb0b0b0",D); D[2]=D[0]; D[3]=y; Polyline(2,D);TextHang(x,y+0.03,0,"Main ring");
x=1.285e8/r_unit;y=1.2;D[0]=x;D[1]=0;D[2]=x;D[3]=y; Polyline(2,D);TextHang(x,y+0.03,0,"Metis,Adrastea");
x=1.81e8/r_unit;y=1.1;D[0]=x;D[1]=0;D[2]=x;D[3]=y; Polyline(2,D);TextHang(x,y+0.03,0,"Amalthea");
x=2.22e8/r_unit;y=1.2;D[0]=x;D[1]=0;D[2]=x;D[3]=y; Polyline(2,D);TextHang(x,y+0.03,0,"Thebe");
SetPen(2,0xff0000);Polyline(n/2,S,5,1.4,"#if|ψ|²#t (density, prediction)"); SetPen(1,0xff);
}#v07=?>A
```

```
<Clet2020 Script>// C source code [8]
char Stars[100]={"#ifr#sds#t;Halo ring;Main ring;Metis,Adrastea;Amalthea;Thebe; ;"};
double r[10]={0.7149,0.92,1.22,1.285,1.81,2.22,0};
double a,b,x,y,dP[10],D[100],S[2000];int i,j,k,N,nP[10];char str[200];
```

```

main(){SetViewAngle(0,50,10);a=3;N=6;
SetAxis(X_AXIS,-a,0,a,"x;");SetAxis(Y_AXIS,-a,0,a,"y;");SetAxis(Z_AXIS,-a,0,a,"z;");
DrawFrame(FRAME_LINE,2,0x00ffff); //SetPen(1,0x808000);
for(i=0;i<N;i+=1) {b=r[i];
D[0]=0;D[1]=0;D[2]=0;D[3]=0;D[4]=1;D[5]=0;D[6]=0;D[7]=0;D[8]=1;
D[9]=600;D[10]=b;D[11]=b;
Lattice(OVAL,D,S);Plot("POLYGON,0,600,XYZ,10",S[9]);
nP[0]=TAKE;nP[1]=i;TextJob(nP,Stars,str);y=r[i];x=0.2; if(i>2) y=-y; TextHang(x,y,0,str);}
a=317.816*5.97237e24; y=30;
for(i=0;i<N;i+=1) {x=r[i]*1e+8;b=sqrt(GRAVITYC*a/x);b=2*PI*x/b; b/=3600;
TextAt(100,y,"i=%d r=%e T=%f",i,x,b); y+=30;}
}#v07=?>A

```

For Saturn, the maxima of $|\psi(r)|^2$ point out the orbital radii of Mimas, Enceladus, Tethys and Dione, respectively; also approximately gives out the locations of ring A,B,C and D; as shown in Figure 5, the overall relative error is about 5%.

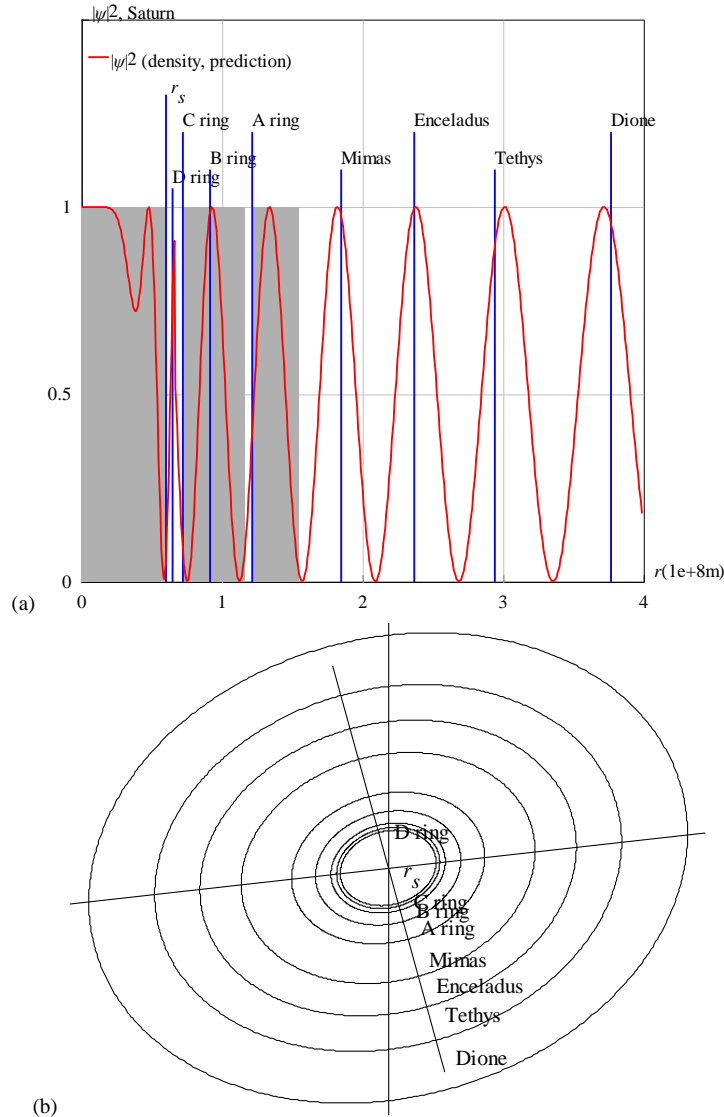


Figure 5 (a) The nucleon distribution $|\psi|^2$ is calculated in the radial direction for Saturn. (b) Orbits

```

<Clet2020 Script>/C source code [8]
int i,j,k,n,N; double H,M,r,r_atm,r_unit,x,y,z,delta,D[10],S[1000];
double rs,rc,omega,amp,d,beta; char str[100];
main(){k=400;rs=9.449*6.378e6; r_atm =rs+rs/10; rc=r_atm; n=0; N=2;
beta=7.175115e+13;H=SPEEDC*SPEEDC*SPEEDC/beta; M=95.16*5.97237e24;
r_unit=4e+8/k; omega=2*PI/(10.6562*60*60); //angular speed
for(i=0;i<k;i+=1) {r=i*r_unit; x=r/rs;
if(r<r_atm) {delta=2*PI*omega*r/H; amp=pow(x,5);}
else {delta=2*PI*sqrt(GRAVITYC*M*r)/H; amp=1;}
d=(1+amp)*(1+amp); x=1+amp*cos(delta); y=amp*sin(delta); z=(x*x+y*y)/d; S[n]=i; S[n+1]=z; n+=2; }
SetAxis(X_AXIS,0,0,k,"#i f#t(1e+8m);0;1;2;3;4;");SetAxis(Y_AXIS,0,0,1.5,"#i f#t#su2#t, Saturn;0;0.5;1;");
DrawFrame(0x0143,2,0xafffaf); SetPen(2,0xff);

```

```

x=rs/r_unit;y=1.3;D[0]=0;D[1]=0;D[2]=x;D[3]=1;
Draw("RECT,3,XY,0,0xb0b0b0",D); D[0]=D[2];D[3]=y; Polyline(2,D);TextHang(x,y+0.03,0," #ifr#sds#t ");
x=0.65e8/r_unit;y=1.05;D[0]=x;D[1]=0;D[2]=x;D[3]=y; Polyline(2,D);TextHang(x,y+0.03,0,"D ring");
x=0.72e8/r_unit;y=1.2;D[0]=x;D[1]=0;D[2]=0.9e8/r_unit;D[3]=1;
Draw("RECT,3,XY,0,0xb0b0b0",D); D[2]=D[0];D[3]=y; Polyline(2,D);TextHang(x,y+0.03,0,"C ring");
x=0.915e8/r_unit;y=1.1;D[0]=x;D[1]=0;D[2]=1.165e8/r_unit;D[3]=1;
Draw("RECT,3,XY,0,0xb0b0b0",D); D[2]=D[0];D[3]=y; Polyline(2,D);TextHang(x,y+0.03,0,"B ring");
x=1.215e8/r_unit;y=1.2;D[0]=x;D[1]=0;D[2]=1.55e8/r_unit;D[3]=1;
Draw("RECT,3,XY,0,0xb0b0b0",D); D[2]=D[0];D[3]=y; Polyline(2,D);TextHang(x,y+0.03,0,"A ring");
x=1.85e8/r_unit;y=1.1;D[0]=x;D[1]=0;D[2]=x;D[3]=y; Polyline(2,D);TextHang(x,y+0.03,0,"Mimas");
x=2.37e8/r_unit;y=1.2;D[0]=x;D[1]=0;D[2]=x;D[3]=y; Polyline(2,D);TextHang(x,y+0.03,0,"Enceladus");
x=2.94e8/r_unit;y=1.1;D[0]=x;D[1]=0;D[2]=x;D[3]=y; Polyline(2,D);TextHang(x,y+0.03,0,"Tethys");
x=3.77e8/r_unit;y=1.2;D[0]=x;D[1]=0;D[2]=x;D[3]=y; Polyline(2,D);TextHang(x,y+0.03,0,"Dione");
SetPen(2,0xff0000); Polyline(n/2,S,5,1.4,"#if|ψ|#su2#t (density, prediction)");
}#v07=?>A

```

```

<Clet2020 Script>// C source code [8]
char Stars[100]={"#ifr#sds#t;D ring;C ring;B ring;A ring;Mimas;Enceladus;Tethys;Dione; ;"};
double r[10]={0.603,0.65,0.72,0.915,1.215,1.85,2.37,2.94,3.77,0.};
double a,b,x,y,dP[10],D[100],S[2000];int i,j,k,N,nP[10];char str[200];
main(){SetViewAngle(0,50,10);a=4;N=9;
SetAxis(X_AXIS,-a,0,a,"x");SetAxis(Y_AXIS,-a,0,a,"y");SetAxis(Z_AXIS,-a,0,a,"z");
DrawFrame(FRAME_LINE,2,0x00ffff); //SetPen(1,0x808000);
for(i=0;i<N;i+=1) {b=r[i]; D[0]=0;D[1]=0;D[2]=0;D[3]=0;D[4]=1;D[5]=0;D[6]=0;D[7]=0;D[8]=1;
D[9]=600;D[10]=b;D[11]=b;
Lattice(OVAL,D,S); Plot("POLYGON,0,600,XYZ,10",S[9]);
nP[0]=TAKE;nP[1]=i;TextJob(nP,Stars,str);y=r[i];x=0.2; if(i>1) y=-y; if(i==0) y=0;
TextHang(x,y,0,str);}
a=95.16*5.97237e24; y=30;
for(i=0;i<N;i+=1) {x=r[i]*1e+8;b=sqrt(GRAVITYC*a/x);b=2*PI*x/b; b/=3600;
TextAt(100,y,"i=%d r=%e T=%f",i,x,b); y+=30;}
}#v07=?>A

```

5. Earth's tidal cycles and ocean circulations

Similar to Jupiter and Saturn, the Earth also has many quantum gravity issues such as the atmosphere and space debris [9-16], that has been discussed in the early paper[1]; this section focuses on the issue of tidal periods and ocean circulations in terms of the planetary-scale relativistic matter wave. To note, the Earth has a mean density of 5530 (kg/m³), the Earth's angular speed is known as $\omega=2\pi/(24 \times 3600)$ (s⁻¹), its mass 5.97237e+24 (kg), the well-known radius is 6.378e+6 (m). The ultimate acceleration on the Earth is $\beta=1.377075e+14$ (m/s²) [1][17].

Tide is a natural phenomenon that occurs in coastal areas, referring to the periodic movement of seawater under the influence of celestial tidal forces. Without considering the weak effects of the sun and other planets, the tidal force of the Moon on the ocean is the cause of seawater fluctuations. Seawater is constantly flowing. Open a current map, you will find that the curves on it, representing the approximate route of seawater flow, as shown in Figure 6(a).

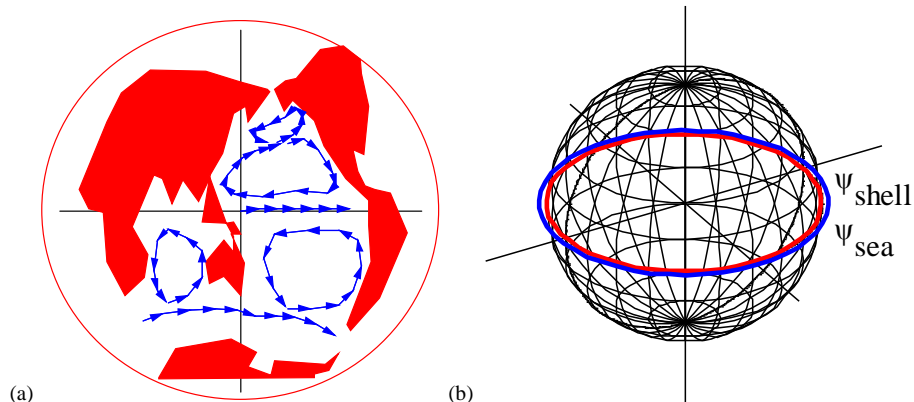


Figure 6 (a) Ocean circulations. (b) The interference between seawater's ψ_{sea} and shell's ψ_{shell} .

```

<Clet2020 Script>// C source code [8]

```

```

int
D[80]={16,66,4,49,3,58,-4,54,-10,32,-17,19,-8,-7,-4,-6,0,-13,-5,-13,2,-29,0,-47,-9,-36,-17,-40,-19,-28,-9,-16,-4,-23,-4,-14,-8,-7,-
21,-6,-17,18,-23,5,-32,17,-38,4,-43,18,-48,20,-60,-9,-51,-24,-53,-37,-64,-47,-74,-28,-76,-1,-84,1,-89,12,-74,49,-66,65,-50,78,-19,
77,0,71,15,67,};
int
D1[54]={19,67,24,55,29,61,41,50,46,36,58,18,71,6,71,-8,72,-28,59,-63,61,-66,77,-48,92,-12,83,10,74,12,69,14,65,22,62,34,68,3
1,71,58,67,76,66,84,57,91,44,89,31,73,25,72,19,67,};
int D2[28]={-45,-92,-36,-76,-5,-71,9,-78,4,-86,17,-91,19,-83,47,-85,54,-79,49,-88,41,-90,41,-92,-45,-93,-45,-93,};
int J1[20]={20,38,29,42,34,48,34,54,30,57,25,52,16,48,7,44,9,39,15,38,};
int J2[30]={26,37,35,40,43,34,51,21,53,14,48,10,31,11,12,8,-3,9,-9,14,-7,20,1,29,8,33,17,35,22,37,};
int J3[20]={-54,-61,-43,-57,-28,-55,-14,-54,-2,-55,8,-58,20,-58,30,-59,42,-63,52,-69,};
int J4[20]={-40,-51,-29,-47,-21,-37,-21,-22,-30,-15,-40,-10,-46,-16,-48,-33,-46,-44,-41,-50,};
int J5[24]={26,-54,39,-54,54,-52,62,-44,67,-31,65,-16,55,-11,37,-11,19,-13,13,-26,18,-43,25,-53,};
int J6[20]={0,0,10,1,20,1,30,1,40,1,50,1,60,1,};
main(){DrawFrame(FRAME_LINE,1,0xffff); SetPen(1,0xffff); Draw("ELLIPSE,0,2,XY,0",-110,-105,110,105");
Plot("POLYGON,3,40,XY,10",D);Plot("POLYGON,3,27,XY,10",D1);Plot("POLYGON,3,14,XY,10",D2);
SetPen(1,0xff);Plot("POLYLINE,5,10,XY,10",J1);Plot("POLYLINE,5,15,XY,10",J2);
Plot("POLYLINE,5,10,XY,10",J3);Plot("POLYLINE,5,10,XY,10",J4);Plot("POLYLINE,5,12,XY,10",J5);
Plot("POLYLINE,5,7,XY,10",J6);
}#v07=?>A

<Clet2020 Script>// C source code [8]
double D[2000], r,x,y,v1,v2,K1,K2; int i,j,k,N;
int main(){SetViewAngle("temp0,theta60,phi-60");
DrawFrame(FRAME_LINE,1,0xffff);Overlook("2,1,60", D); r=60;
for(i=0;i<180;i+=15) {k=0; K1=0; K2=i;Grid();}
for(i=0;i<180;i+=15) {k=1; K1=i; K2=0;Grid();}
SetPen(3,0xffff);k=1; K1=90; K2=0; Grid();
SetPen(3,0x00ff);r=63; K1=90; K2=0; Grid();
TextHang(10,70,0,"ψ#sdshell##t#nψ#sdsea"); }
Grid(){N=50; K1*=PI/180; K2*=PI/180;
if(k==0) {v1=2*PI/N; v2=0;} else {v1=0; v2=2*PI/N;}
for(j=0;j<=N;j+=1){ k=j+j;
D[k]=r*sin(K1)*cos(K2);D[k+1]=r*sin(K1)*sin(K2); D[k+2]=r*cos(K1);
K1+=v1;K2+=v2; }Plot("POLYGON,0,50, XYZ,10",D);
}#v07=?>A #t

```

The seawater over Earth's shell is subject to the interference between seawater's ψ_{sea} and shell's ψ_{shell} , as illustrated in Figure 6(b) at the equator. In the Earth-orbital frame of reference, consider a point at latitude angle A , according to Eq.(1), the generalize matter waves are given by

$$\begin{aligned}
\psi(r, A) &= \psi_{sea} + C\psi_{shell} \\
\psi_{sea} &= \exp\left[\frac{i\beta}{c^3} \int_0^x v_{sea} dl + \frac{i\beta}{c^3} \int_0^t \left(\frac{-c^2}{\sqrt{1-v_{sea}^2/c^2}}\right) dt\right] \\
\psi_{shell} &= \exp\left[\frac{i\beta}{c^3} \int_0^x v_{shell} dl + \frac{i\beta}{c^3} \int_0^t \left(\frac{-c^2}{\sqrt{1-v_{shell}^2/c^2}}\right) dt\right]
\end{aligned} \tag{7}$$

where C is the coupling constant. The interference between seawater's ψ_{sea} and shell's ψ_{shell} would produce a beat phenomenon [1]:

$$\begin{aligned}
\frac{2\pi}{\lambda_{beat}} &= \frac{\beta}{c^3} (v_{sea} - v_{shell}); & \frac{2\pi}{T_{beat}} &= \frac{\beta}{2c^3} (v_{sea}^2 - v_{shell}^2) \\
v_{sea} &= \omega r \cos A + v_{flow} + v_{tide_effect} \\
v_{shell} &= r\omega
\end{aligned} \tag{8}$$

The Moon exerts a tidal force on the seawater, which is represented by the quantity v_{tide_effect} in the above equations; v_{tide_effect} is not true movement but only equivalents to the tide effect. Sea flow from west to east is defined as positive flow in the followings. The shell's ψ_{shell} has spherical symmetry because the Earth's matter density has a spherical symmetry: $\rho(r,A,\varphi)=\rho(r)$ in this model, i.e. it has experienced a spheroidization process for a long term evolution before it becomes a spheroid, therefore ψ_{shell} is calculated at any point within the equator with the speed $v_{shell}=r\omega$. The beat period in the seawater is under the control of the Moon's period,

that is

$$T_{beat} = \frac{4\pi c^3}{\beta[(\omega r \cos A + v_{flow} + v_{tide_effect})^2 - (r\omega)^2]} \approx 27.32(days) \quad (9)$$

Solving for the flow, it is written as

$$v_{flow} = \sqrt{\omega^2 r^2 + \frac{4\pi c^3}{\beta T_{beat}} - \omega r \cos(A) - v_{tide_effect}} \quad (10)$$

Thus, Earth's beat phenomenon is characterized in terms of the interference of the generalized matter waves as follows.

(1) Forced oscillation of seawater by the tide

Analyzing the experimental observations of tides and ocean circulations, we know that the overall tide effect would exert a tidal force on the seawater within the equator with a beat period of 27.32 days, and the sea-flows near the equator run at a speed of about 1 m/s. Substituting $T_{beat}=27.32$ days and $v_{flow}=1$ m/s at the latitude $A=0$ into the above equation, we obtain a value of the tide effect: $v_{tide_effect}=656.58$ m/s. At other latitude A , we should take into account the inclination factor for the tide effect, as shown in Figure 7. The Moon has an orbit with a large tilt with respect to the Earth's equator. The Moon's orbit is tilted between 18° and 29° with respect to the Earth's equator. Averagely, the tide effect to the Earth has the most strong influence to latitudes at about 30°N on the north hemisphere. Therefore, after fitting experimental data, the global tide effect at different latitude A is suggested to be

$$v_{tide_effect} = 656.58(1 + \sin |A + A/3|) \quad (m/s) \quad (11)$$

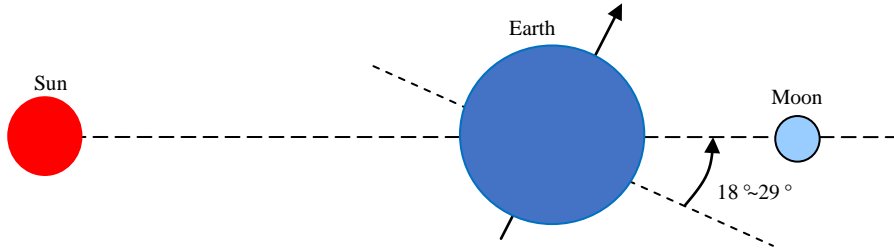


Figure 7 The Moon's orbit is tilted between 18° and 29° with respect to the Earth's equator.

On the Earth surface, the belt with zero-flow is called as the coherent ridge (interference constructive ridge), the location at the equator $A=0$ is usually considered to be the first coherent ridge.

(2) Seawater flows required for coherence

Seawater is calm at coherent ridge with zero-speed, while slowly flows nearby. Substituting the global tide effect into the above beat period formula, the flows under the control of the beat T_{beat} nearby can be determined. The flows required for the first beat period $T_1=27.32$ days nearby is calculated by the above equation, as shown in Figure 8 (the blue line near $A=0$). The maximal flow speed is constricted by its neighboring ridges, is estimated as 1 m/s.

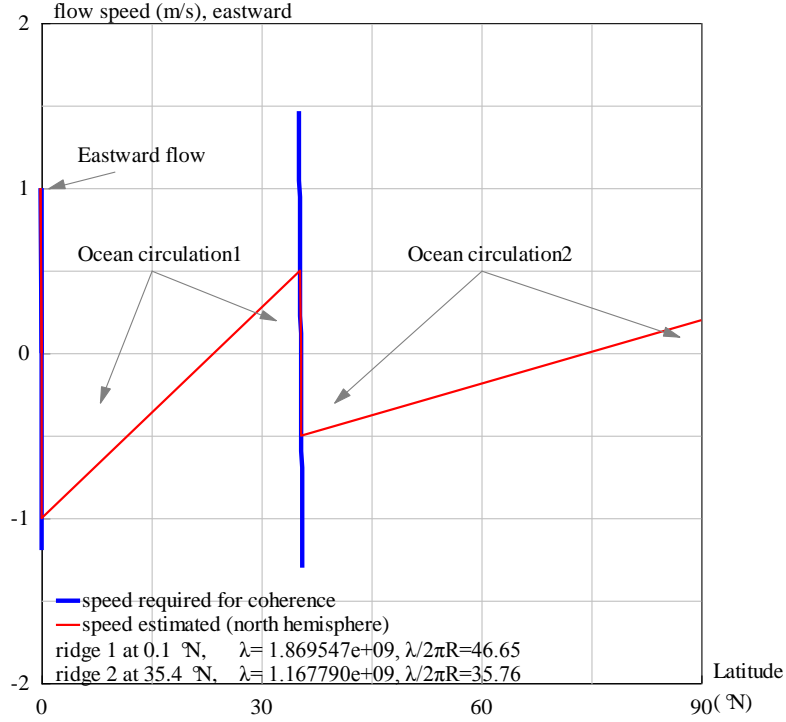


Figure 8 Sea-flow speeds in the north hemisphere of the Earth.

```

<Clet2020 Script>// C source code [8]
double beta,H,M,r,rs,omega,v1,v2,V,V1,V2,T,T1,a,b,c,d,w,Fmax, N[1000],S[1000],F[20],D[20],U[10],X,Y;
int i, j, k, N1, m, n, s, f;
int main(){beta=1.377075e+14; H=SPEEDC*SPEEDC*SPEEDC/beta;
M=5.97237e24; rs=6.378e6; omega=2*PI/(24*3600); T1=27.3*24*3600;
v2=rs*omega; Fmax=1; a=v2*v2+4*PI*H/T1; V=sqrt(a)-v2-Fmax; b=(v2+V+v2)/2;d=sqrt(4*PI*H/T1);
V1=2; V2=-2; SetAxis(X_AXIS,0,0,90,"Latitude#n(° N);0;30;60;90;");
SetAxis(Y_AXIS,V2,V2,V1,"flow speed (m/s), eastward;-2;-1;0;1;2;");
DrawFrame(0x0168,2,0xfffffff); TextHang(5,1.8,0,"V=% .2f,v2=% .2f, b=% .2f, d=% .2f ",V,v2,b,d);
SetPen(4,0xff); f=0; m=0; V1=1.5; V2=-1.4; X=2; Y=-1.5;
for(j=1;j<4;j+=1) { T=T1/j; Wind(); Polyline(n,N); }
Polyline(2,F,X,Y,"speed required for coherence");Y=-0.15;
SetPen(2,0xffff0000);F[f+f]=90;F[f+f+1]=0.2;f+=1;Polyline(f,F);
Polyline(2,F,X,Y,"speed estimated (north hemisphere)");Y=-0.15;X=2;//Y=-0.15;
for(i=0;i<m;i+=1) {a=U[i+1];TextHang(X,Y,0,"ridge #d at % .1f °N",i+1,a);//Y=15;
a=a*PI/180; b=(U[i+1]+v2)/2; c=b*T1/(i+1); d=b/(2*PI*rs*cos(a));
TextHang(X+25,Y,0,"λ = %e, λ/2πR=% .2f",b,c);Y=-0.15; }
SetPen(1,0xafaf5f);D[0]=ARROW;D[1]=0;D[2]=2;D[3]=XY;D[4]=15;
TextHang(5,0.6,0,"Ocean circulation1"); Draw(D,"15,0.5,8,-0.3,");Draw(D,"15,0.5,32,0.2,");
TextHang(50,0.6,0,"Ocean circulation2"); Draw(D,"60,0.5,40,-0.3,");Draw(D,"60,0.5,87,0.1,");
TextHang(5,1.2,0,"Eastward flow");Draw(D,"10,1.1,1,1,");
}
Wind(){n=0; s=0; N1=5000; c=PI/(N1+N1); v2=omega*rs; a=v2*v2+4*PI*H/T; d=sqrt(a);
for(i=0;i<N1/2;i+=1) { a=i*c; v1=omega*rs*cos(a); w=d-v1-V*(1+sin(a+a/3));
if(w>V2 && w<V1) {N[n+n]=a*180/PI; N[n+n+1]=w; S[n+n]=w; S[n+n+1]=N[n+n];n+=1; }
}
//-----
if(n==0) return; D[0]=TREND; D[1]=n;
w=Fmax/j;D[2]=w; DataJob(D,S,a); F[f+f]=a;F[f+f+1]=w; f+=1;
w=0;D[2]=w; DataJob(D,S,a); F[f+f]=a;F[f+f+1]=w; f+=1; U[m+m]=a; U[m+m+1]=d; m+=1;
w=-Fmax/j;D[2]=w; DataJob(D,S,a); F[f+f]=a;F[f+f+1]=w; f+=1;
}#v07=?>A

```

(3) Coherent ridges

As the latitude A rises, the first coherent ridge will be destroyed due to destructive interference, but, the generalized matter waves will again satisfy the constructive interference condition at higher latitudes. Other coherent ridges will form at different latitudes with different beat periods; such as the second coherent ridge with $T_2=T_1/2$, ..., until into the polar regions. Calculation of the coherent ridges and sea-flow speeds are carried out in Figure 8. Gap between two neighboring coherent ridges has stronger shear-flows. The predicted flow-curve in the north hemisphere agrees well qualitatively with the experimental

observations for the ocean circulations.

(4) Beat wavelength and tide

According to the calculation, the beat wavelength λ of the first coherent ridge is longer than the equatorial circumference by many times, $\lambda/2\pi R=46.65$, where $R=r\cos(A)$. This situation does not mean that the beat will vanish for imagined destructive interference. At the first, the closed circumference used in the calculation should relax to adapt its real interference requirement so that the ratio should take an integer: $[\lambda/2\pi R]=47$. Next, one beat wavelength λ wraps up the real circumference by 47 cycles, as illustrated in Figure 9(a), the overlapped beat-wave at any point of the circumference should take the sum, similar to the Fabry-Perot interference formula in optics, that is

$$\psi = \psi_0(1 + e^{i\delta} + e^{i2\delta} + e^{i3\delta} + \dots + e^{i(N-1)\delta}) = \frac{1 - \exp(iN\delta)}{1 - \exp(i\delta)} \psi_0$$

$$1st_ridge: \delta = \frac{2\pi}{47}, N = 47, (\text{with one peak around Earth}) \quad (12)$$

$$2nd_ridge: \delta = \frac{2\pi}{36}, N = 2 \times 36 = 72, (\text{with two peaks around Earth})$$

In the Earth-orbital frame of reference, the intensity of $|\psi|^2$ represents the height of sea level, i.e. $|\psi|^2$ expresses the tidal wave-form, it has one maximal peak and 45 billows on the circumference within the equator with a beat period $T_1=27.32$ days; the second ridge at the latitude 35.4°N has two maximal peaks and 2×34 billows on its circumference with a beat period $T_2=T_1/2=18.66$ days, as illustrated in Figure 9(b). The intensity curves of $|\psi|^2$ around the Earth are illustrated in Figure 9(c).

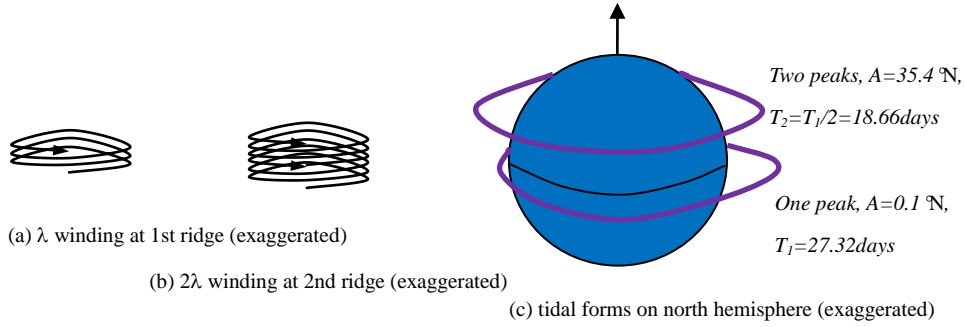


Figure 9 $|\psi|^2$ expresses the tidal wave-form, it has one maximal peak around the circumference within the equator with a beat period $T_1=27.32$ days; the second ridge at the latitude 35.4°N has two maximal peaks around the circumference with a beat period $T_2=T_1/2=18.66$ days.

The width of the equatorial tidal peak and its lasting time are calculated by

$$w_{peak} = 2 \times \frac{2\pi r}{46} = 1741(\text{km}); \quad Time_{peak} = \frac{w_{peak}}{r\omega} = 1.04(\text{hours}) \quad (13)$$

Measured by Earth-observer, the period of tide within the equator, i.e. the lunar day, T_{tide} is calculated by

$$\frac{2\pi r}{T_{tide}} \approx \frac{2\pi r}{T_{earth}} - \frac{2\pi r}{T_{moon}}; \Rightarrow T_{tide} \approx 24.91(\text{hours}) . \quad (14)$$

For observer on the Earth surface, in the vicinity of the first ridge $A=0.1^\circ \text{N}$, he or she will count one tidal peak per 24.91 hours (**full day tide**). In the vicinity of the second ridge $A=35.4^\circ \text{N}$, he or she will count one tidal peak per 12.45 hours (there are two peaks for $|\psi|^2$ on its circumference around the Earth), (**half day tide**). This prediction agrees well with the tidal observations at ports around the world in Table 1 and Table 2.

Table 1 Components of tides measured at four ports, March,1936 [18].

Port	Latitude	Amplitude/ Half day tide	Amplitude/ Full day tide	Ratio
Immingham, Scotland	53 °N	223cm	15 cm	14.86
San Francisco, USA	37 °N	54 cm	37 cm	1.56
Manila, Philippine	15 °N	20 cm	30 cm	0.67
TuShan, Vietnam	20 °N	4 cm	72 cm	0.056

Table 2 Components of tides measured at ports of China [18].

Port	Latitude	Amplitude/ Half day tide	Amplitude/ Full day tide	Ratio
Yingkou	40.6 °N	117cm	33 cm	3.54
Dalian	38.9 °N	99 cm	27 cm	3.67
Dagu	39 °N	94 cm	25 cm	3.76
Yantai	37.4 °N	74 cm	18 cm	4.11
Weihai	37.5 °N	59 cm	22 cm	2.68
Chengshanjiao	37.3 °N	20 cm	23 cm	0.87
Qingdao	36 °N	125 cm	27 cm	4.63
Wusongkou	31.2 °N	95 cm	20 cm	4.75
Xiamen	24.5 °N	187 cm	27 cm	6.93
Jirong	25.1 °N	79 cm	19 cm	4.16
Gaoxiong	22.6 °N	20 cm	20 cm	1
Shantou	23.3 °N	42 cm	29 cm	1.45
Hongkong	22.2 °N	44 cm	37 cm	1.19
Beihai	21.5 °N	39 cm	102 cm	0.38

(5) Ocean circulations

On the north hemisphere, the ocean circulations are mainly dominated by the first coherent ridge and second coherent ridge. In Figure 8, the equatorial belt has an eastward seawater flow at the speed about 1m/s; between 0.1°N and 35.4°N there is a larger ocean circulation; between 35.4°N and 90°N there is another ocean circulation. In fact, other coherent ridges at higher latitudes have been blocked by the several continents. The prediction agrees well qualitatively with the experimental observations for the ocean circulations.

(6) Other factors

As we known, solar attraction acting on the Earth also have impact on the tides and ocean circulations. In addition, Coriolis effect, sea beds and continents also have important influences on the motion of the Earth's seawater. These factors are usually regarded as secondary smaller quantities, and are neglected in the present model.

6. Jupiter's zonal winds

The clouds over Jupiter's shell form well-observed belts and zones, are subject to the interference between cloud's ψ_{cloud} and shell's ψ_{shell} , as illustrated in Figure 10 at the equator.

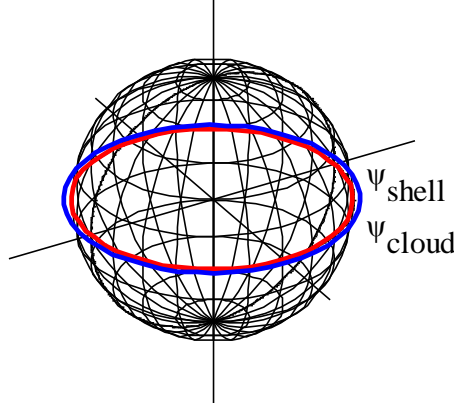


Figure 10 The interference between shell's ψ_{shell} and cloud's ψ_{cloud} .

```
<Clet2020 Script>// C source code [8]
double D[2000], r,x,y,v1,v2,K1,K2; int i,j,k,N;
int main(){SetViewAngle("temp0,theta60,phi-60");
DrawFrame(FRAME_LINE,1.0xaffaf);Overlook("2,1,60", D); r=60;
for(i=0;i<180;i+=15) {k=0; K1=0; K2=i;Grid();}
for(i=0;i<180;i+=15) {k=1; K1=i; K2=0;Grid();}
SetPen(3,0xff0000); k=1; K1=90; K2=0; Grid();
SetPen(3,0x00ff);r=63; K1=90; K2=0; Grid();
TextHang(10,70,0,"ψ#sdshell#t#nψ#sdcloud"); }
Grid(){N=50; K1*=PI/180; K2*=PI/180;
if(k==0) {v1=2*PI/N; v2=0;} else {v1=0; v2=2*PI/N;}
for(j=0;j<=N;j+=1){ k=j+j+j;
D[k]=r*sin(K1)*cos(K2);D[k+1]=r*sin(K1)*sin(K2); D[k+2]=r*cos(K1);
K1+=v1;K2+=v2; }Plot("POLYGON,0,50, XYZ,10",D);
}#v07=?>A #t
```

In the Jupiter-orbital frame of reference, consider a point at latitude angle A , according to Eq.(1), the generalize matter waves are given by

$$\begin{aligned}\psi(r, A) &= \psi_{cloud} + C\psi_{shell} \\ \psi_{cloud} &= \exp\left[\frac{i\beta}{c^3} \int_0^x v_{cloud} dl + \frac{i\beta}{c^3} \int_0^t \left(\frac{-c^2}{\sqrt{1-v_{cloud}^2/c^2}}\right) dt\right] \\ \psi_{shell} &= \exp\left[\frac{i\beta}{c^3} \int_0^x v_{shell} dl + \frac{i\beta}{c^3} \int_0^t \left(\frac{-c^2}{\sqrt{1-v_{shell}^2/c^2}}\right) dt\right]\end{aligned}\quad (15)$$

where C is the coupling constant. The interference between cloud's ψ_{cloud} and shell's ψ_{shell} would produce a beat phenomenon [20]:

$$\begin{aligned}\frac{2\pi}{\lambda_{beat}} &= \frac{\beta}{c^3} (v_{cloud} - v_{shell}); \quad \frac{2\pi}{T_{beat}} = \frac{\beta}{2c^3} (v_{cloud}^2 - v_{shell}^2) \\ v_{cloud} &= \omega r \cos A + v_{wind} + v_{tide_effect} \\ v_{shell} &= r\omega\end{aligned}\quad (16)$$

The Jupiter's satellites (Metis, Adrastea, Amalthea, Thebe, etc.) exert a tidal force on the clouds, which is represented by the quantity v_{tide_effect} in the above equation; v_{tide_effect} is not true movement but only equivalents to the overall tide effect. West wind from west to east is

defined as positive wind in the followings. The shell's ψ_{shell} has spherical symmetry because the matter density has a spherical symmetry: $\rho(r,A,\varphi)=\rho(r)$ in this model, i.e. it has experienced a spheroidization process for a long term evolution before it becomes a spheroid, therefore ψ_{shell} is calculated at any point within the equator with the speed $v_{shell}=r\omega$. The beat period is given by

$$T_{beat} = \frac{4\pi c^3}{\beta[(\omega r \cos A + v_{wind} + v_{tide_effect})^2 - (r\omega)^2]} . \quad (17)$$

Solving for the wind, it is written as

$$v_{wind} = \sqrt{\omega^2 r^2 - \frac{4\pi c^3}{\beta T_{beat}}} - \omega r \cos(A) - v_{tide_effect} . \quad (18)$$

Thus, Jupiter's beat phenomenon is characterized in terms of the generalized matter waves as follows.

(1) Forced oscillation by the tide

Analyzing the experimental observations in the recent Juno and Cassini missions, we know that the overall tide effect would exert a tidal force on clouds within the equator with a beat period of 82 hours where the interference causes almost zero-winds within the equator. Substituting $T_{beat}=82$ hours and $v_{wind}=0$ at the latitude $A=0$ into the above equation, we obtain a value of the tide effects: $v_{tide_effect}=-1193.1$ m/s. At other latitude A , we should take into account the inclination factor for the tide effect, the global tide effect is suggested to be

$$v_{tide_effect} = -1193.1 \cos A \quad (m/s) . \quad (19)$$

On the Jupiter's surface, the belt with zero-wind is called as the coherent ridge (interference constructive ridge), the location at the equator $A=0$ is usually considered to be the first coherent ridge.

(2) Winds required for coherence

Cloud is calm at the coherent ridge, while blows breeze winds nearby. Substituting the global tide effect into the above beat period formula, the wind under the control of the beat T_{beat} nearby can be determined. The wind required for the first beat period $T_1=82$ (hours) nearby is calculated by the above equation, as shown in Figure 11 (the blue line near $A=0$). The maximal wind is constricted by its neighbor ridges, is estimated as 120 m/s.

(3) Other coherent ridges

As the latitude A rises, the first coherent ridge will be destroyed due to destructive interference, but, the waves will again satisfy the constructive interference condition at higher latitudes. Other coherent ridges will form at different latitudes with different beat periods, the second coherent ridge with $T_2=T_1/2$; the third coherent ridge with $T_3=T_1/3, \dots$, until into the polar regions. Calculation of the coherent ridges and wind speeds are carried out in Figure 11. Gap between two neighboring coherent ridges has stronger shear-winds. The predicted wind-curve in the south hemisphere agrees well qualitatively with the experimental observations [20][21].

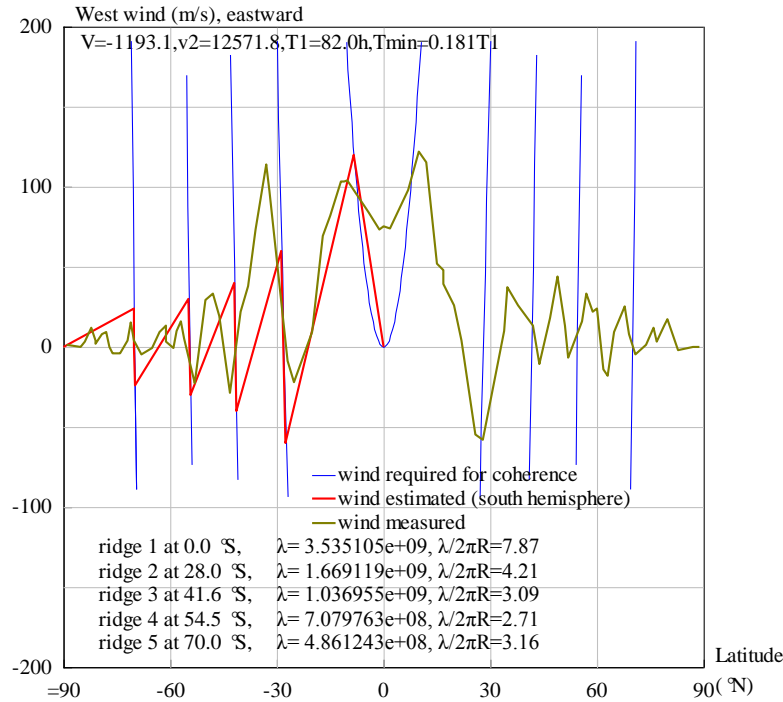


Figure 11 Calculation of zonal winds in the south hemisphere of Jupiter.

```

<Clet2020 Script>// Jupiter C source code [8]
double beta,H,M,r,rs, omega,v1,v2,V,V1,V2,T,T1,T2,a,b,c,d,w,Fmax, N[500],S[500],F[100],D[20];
int i, j, k, X, Y, m, n, s, f;
int ZonalWind[166]={
-89,1,-85,0,-84,3,-82,12,-82,12,-81,4,-81,2,-79,8,-78,9,-77,0,-76,4,-74,-4,-72,4,-71,15,-70,4,-68,-5,-65,-1,-63,9,-61,13,-61,3,-59,-
1,-58,10,-57,16,-56,5,-53,-23,-50,29,-48,33,-46,19,-43,-29,-40,22,-38,38,-36,73,-33,114,-32,97,-27,-9,-25,-22,-20,9,-17,69,-15,82
,-12,103,-11,103,-10,104,-4,84,-1,73,0,75,2,74,7,98,10,122,12,115,15,52,17,48,17,39,20,26,22,4,26,-55,28,-58,34,10,35,37,38,26
,42,13,44,-11,47,18,49,44,51,13,52,-7,56,16,57,33,59,22,60,24,62,-14,63,-18,65,9,68,25,69,8,71,-5,74,1,76,12,77,3,79,13,80,17,8
3,-2,87,0,89,0,
};
int main(){beta=4.013970e+13; H=SPEEDC*SPEEDC*SPEEDC/beta;
M=317.816*5.97237e24; rs=11.209*6.378e6; omega=2*PI/(9.925*3600); T1=82*3600;
v2=rs*omega; Fmax=120; a=v2*v2-4*PI*H/T1; V=sqrt(a)-v2; T2=4*PI*H/v2*v2; T2=T2/T1;
V1=200; V2=-V1; SetAxis(X_AXIS,-90,-90,90,"Latitude#n(°N)"); SetAxis(Y_AXIS,-100,100,200,"");
DrawFrame(0x0168,2,0xffff); TextHang(-85,190,0,"V=%1f,v2=%1f,T1=%1fh,Tmin=%1fT1",V, v2,T1/3600,T2);
SetPen(1,0xff); f=0; m=0; V2=-V1/2; X=-20; Y=-80;
for(j=1;j<10;j+=1) { T=T1/j; Wind(); Polyline(n,N); Polyline(s,S); }
Polyline(2,S,X,Y,"wind required for coherence"); Y=15;
SetPen(2,0xffff00); F[f+f]=90; F[f+f+1]=0; f+=1; Polyline(f,F);
Polyline(2,F,X,Y,"wind estimated (south hemisphere)"); Y=15;
SetPen(2,0xafaf00); Polyline(83,ZonalWind); Polyline(2,F,X,Y,"wind measured"); X=-80; Y=15;
for(i=0;i<m;i+=1) { a=-D[i+1]; TextHang(X,Y,0,"ridge %d at %1f S",i+1,a)/Y=15;
a=a*PI/180; v1=(v2+D[i+1])/2; b=v1*T1/(i+1); c=b/(2*PI*rs*cos(a));
TextHang(X+50,Y,0,"λ= %e, λ/2πR=%1f",b,c); Y=15; }
}
Wind(){n=0; s=0; c=PI/360; v2=omega*rs; a=v2*v2-4*PI*H/T; d=sqrt(a);
for(i=0;i<180;i+=1) { a=i*c; w=d-omega*rs*cos(a)-V*cos(a);
if(w>V2 && w<V1) { N[n+n]=i/2; N[n+n+1]=w; n+=1; } }
for(i=0;i<180;i+=1) { a=-i*c; w=d-omega*rs*cos(a)-V*cos(a);
if(w>V2 && w<V1) { S[s+s]=i/2; S[s+s+1]=w; s+=1; } }
//-----
if(n==0) return; c=180/PI;
w=-Fmax/j;a=(d-w)/(v2+V); b=-acos(a)*c; if(j==1) {b=0;w=0;} F[f+f]=b;F[f+f+1]=w; f+=1;
w=0;a=(d-w)/(v2+V); b=-acos(a)*c; if(j==1) {b=0;w=0;} F[f+f]=b;F[f+f+1]=w; D[m+m]=b; D[m+m+1]=d; m+=1; f+=1;
w=Fmax/j;a=(d-w)/(v2+V); b=-acos(a)*c; F[f+f]=b;F[f+f+1]=w; f+=1;
}
#v07=?>A

```

(4) Beat wavelength and tide

According to the calculation, the beat wavelength λ of the first coherent ridge is longer than the equatorial circumference by many times, $\lambda/2\pi R=7.9$, where $R=r\cos(A)$. This situation does not mean that the beat will vanish for imagined destructive interference. At the first, the closed circumference in the calculation should relax to adapt its real interference requirement so that the ratio should take an integer: $[\lambda/2\pi R]=8$. Next, one beat wavelength λ

wraps up the real circumference by 8 cycles, so that the overlapped beat-wave at any point of the circumference should take the sum, similar to the Fabry-Perot interference formula in optics, that is

$$\psi = \psi_0(1 + e^{i\delta} + e^{i2\delta} + e^{i3\delta} + \dots + e^{i(N-1)\delta}) = \frac{1 - \exp(iN\delta)}{1 - \exp(i\delta)} \psi_0 \quad (20)$$

$$\delta = \frac{2\pi}{8}, N = 8$$

In the Jupiter-orbital frame of reference, the intensity of $|\psi|^2$ expresses the density of the clouds, this intensity curve over the circumference around the equator is illustrated in Figure 12. Theoretically, the circumference consists of 7 gusts of winds, with one maximal peak and 6 secondary billows.

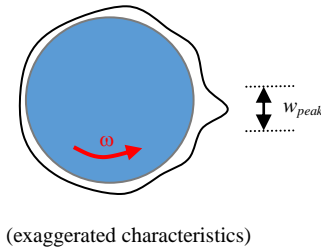


Figure 12 The circumference consists of 7 gusts of winds, with one maximal peak and 6 secondary billows.

To note that $r=71492\text{km}$, $T=9.925\text{h}$, the width of the equatorial tidal peak and its lasting time are given by

$$w_{peak} = 2 \times \frac{2\pi r}{7} = 128277(\text{km}); \quad \text{Time}_{peak} = \frac{w_{peak}}{r\omega} = 2.84(\text{hours}) \quad (21)$$

7. The Great Red Spot on Jupiter

The best known feature in the atmosphere is undoubtedly the Great Red Spot. It is a persistent storm, which has been observed since at least 1831. It rotates in an anticlockwise direction with a rotation period of about 6 days and is thought to be stable and so has become a permanent. It is not, however, fixed in position, and though staying at latitude 22° south, has moved around the planet several times since it was first observed [19].

According to the calculation in the preceding section, on the south hemisphere as shown Fig 11, the Jupiter's south first ridge and second ridge locate at 0°S and 28°S , respectively; the Great Red Spot forms at a location between the two ridges but close to the second ridge; there are two zero-wind points: 28°S and 18°S , thus we predict that

$$A_{Great_Red_Spot} = \frac{18 + 28}{2}^\circ\text{S} = 23^\circ\text{S} \quad (22)$$

$$\text{Size}_{Great_Red_Spot} = (28 - 18)^\circ\text{S} = 10^\circ\text{S}$$

It agrees well with the experimental observation of $\sim 22^\circ\text{S}$, Great Red Spot is a large counter-clockwise vortex on the south hemisphere, whose mature size of 10°S is confined by

the first ridge and second ridge without extra energy to escape. Its stable mechanism is another story by invoking the Planck-constant-like constant [17].

8. Quantum entanglement phenomenon in polar regions

The nature and structure of the observed eastward flows on Jupiter and Saturn have been a long-standing mystery in planetary science. In Figure 11, there are five coherent ridges on the south hemisphere with the beat periods $T_1=82\text{h}$, $T_1/2$, $T_1/3$, $T_1/4$ and $T_1/5$, respectively; the sixth ridge near the south regions can never fulfill in the mathematics on the present conditions, because the expected beat $T_6=T_1/6=0.166T_1$ does not satisfy

$$\sqrt{\omega^2 r^2 - \frac{4\pi c^3}{\beta T_{beat}}} \geq 0 \Rightarrow T_{beat} \geq 0.181T_1 . \quad (23)$$

Thus the fifth ridge with the beat $T_{fifth}=T_1/5$ dominates the whole south polar regions where five storms almost-constantly live around the pole, as illustrated in Figure 13.

But the sixth storm on the south polar regions does has a chance to emerge. We must admit that the mathematically shortest beat $T_{min}=0.181T_1$ would mix its neighboring waves to adapt with its coherent condition, i.e. their entanglement is given by

$$\psi_{0.181T_1} = a\psi_{T_1/5} + b\psi_{T_1/6} . \quad (24)$$

As consequence of the entanglement, an extra stream will burst out from the south pole with the beat period T_{stream} as

$$\frac{1}{T_{stream}} = \frac{1}{T_1/6} - \frac{1}{T_{0.181T_1}} \Rightarrow T_{stream} = 2.1T_1 . \quad (25)$$

Every duration $T_{stream}=2.1T_1$, the extra stream after the emerging of the sixth storm can be observed according to the theory. This consequence is called as the **quantum entanglement phenomenon** in polar regions. Of cause, due to the asymmetry of Jupiter, it is acceptable that eight storms live constantly around the pole in the north polar regions.

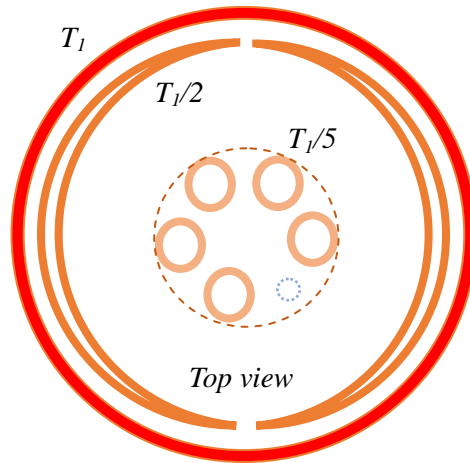


Figure 13 Top view of the south pole of Jupiter. Five storms plus a new storm around the south pole.

As shown in Figure 13, The first beat T_1 wraps up the Jupiter's equator; the second beat $T_1/2$ have been depressed on the surface of the Jupiter at the latitude $28^\circ S$; the fifth beat $T_1/5$ has stretched out to become five storms on the south polar regions; the emergence of sixth beat depends on the process of quantum entanglement in Eq.(24).

Now we come back to the Earth, to say a story that probably is similar to Jupiter: the quantum entanglement phenomenon occurs year in year out in the north polar regions on the Earth. In the arctic region of Earth [1], the third beat $T_{beat}=0.39$ (years) conflicts with the expected well-quantized beat $T_{beat}=1/3$ (years)=0.3333 (years), their entanglement produces a extra cold stream with a beat period

$$\frac{1}{T_{stream}} = \frac{1}{T_{0.3333y}} - \frac{1}{T_{0.39y}} . \quad (26)$$

The cold streams initially go down as easterlies across the west wind zone between the third ridge and second ridge, finally arrive at the equatorial zone and become oscillating winds in the southeast mode or southwest mode alternatively. The 70--10 hPa monthly mean zonal wind, observed at Singapore in Asia [22], which indicates that the cold streams reach equatorial vicinity with an oscillating period of 2.24(years). The above theoretical prediction is just $T_{stream} = 2.24$ (years), which agrees with the observed cycles of the quasi-biennial oscillation in the equatorial lower stratosphere.

The cold streams leaving arctic regions must have a speed that is strong enough to swim bravely across the west wind zone between the third ridge and second ridge at 200hPa altitude (10km), go along with the Hadley cell and Ferrel cell in atmospheric circulations, finally arrive at the equatorial zone with a speed that is strong enough to cope with the equatorial easterlies at 200hPa altitude (10km). Therefore, we estimate that the cold streams leaving arctic regions must have a speed of 20m/s, and have a speed of 10m/s at the equatorial zone. It does not mean that the cold streams will collide with the west winds directly, because their main streams may flow at different altitudes in the sky, their strengths should be of the same order of magnitude. The cold streams go down toward the south as scattering waves, dissipates themselves off in the journey.

9. Saturn's zonal winds

The Saturn's satellites (Mimas, Enceladus, Tethys, Dione, etc.) exert a tidal force on its clouds, which is represented by the quantity v_{tide_effect} in the above beat equation; v_{tide_effect} is not true movement but only equivalents to the overall tide effect. The observation indicates that the overall tide effect would produce a beat period of 81 hours, and causes almost zero-winds within the equator. Substituting $T_{beat}=81$ hours and $v_{wind}=0$ at the latitude $A=0$ into the above beat equation, we obtain a value of the tide effects: $v_{tide_effect}=-856.9$ m/s. At other latitude A , we should take into account the inclination factor for the tide effect, thus the global tide effect is suggested to be

$$v_{tide_effect} = -856.9 \cos A \quad (m/s) . \quad (27)$$

On the Saturn's surface, the belt with zero-wind is called as the coherent ridge (or interference constructive ridge), the location of the equator $A=0$ is the first coherent ridge.

Substituting the global tide effect into the above beat period formula, the wind under the control of the beat T_{beat} nearby the coherent ridge is given by

$$v_{wind} = \sqrt{\omega^2 r^2 - \frac{4\pi c^3}{\beta T_{beat}}} - \omega r \cos(A) - v_{tide_effect} . \quad (28)$$

The wind required for the first coherent beat period $T_1=81$ (hours) nearby is calculated by the above equation, as shown in Figure 14 (the blue line near $A=0$). The maximal wind is constricted by its neighboring ridges, is estimated as 420 m/s.

As the latitude A rises, the first coherent ridge will be destroyed due to destructive interference, but, the waves will again satisfy the constructive interference condition at higher latitudes. Other coherent ridges will form at different latitudes with different beat periods, the second coherent ridge with $T_2=T_1/2$; the third coherent ridge with $T_3=T_1/3, \dots$, until into the polar regions. Calculation of the coherent ridges and wind speeds are carried out in Figure 14. The predicted wind-curve on the south hemisphere agrees well qualitatively with the experimental observations [20][23].

In Figure 14, there are six coherent ridges on the south hemisphere with the beat periods $T_1=81h, T_1/2, T_1/3, T_1/4, T_1/5$ and $T_1/6$, respectively; the seventh coherent ridge near the south regions can never fulfill in the mathematics on the present conditions, because the expected beat $T_7=T_1/7=0.143T_1$ does not satisfy

$$\sqrt{\omega^2 r^2 - \frac{4\pi c^3}{\beta T_{beat}}} \geq 0 \Rightarrow T_{beat} \geq 0.166T_1 . \quad (29)$$

Thus the sixth ridge with the beat period of $T_{sixth}=T_1/6$ dominates the whole south polar regions where the circle of six-sides almost-constantly live around the pole, as we have known.

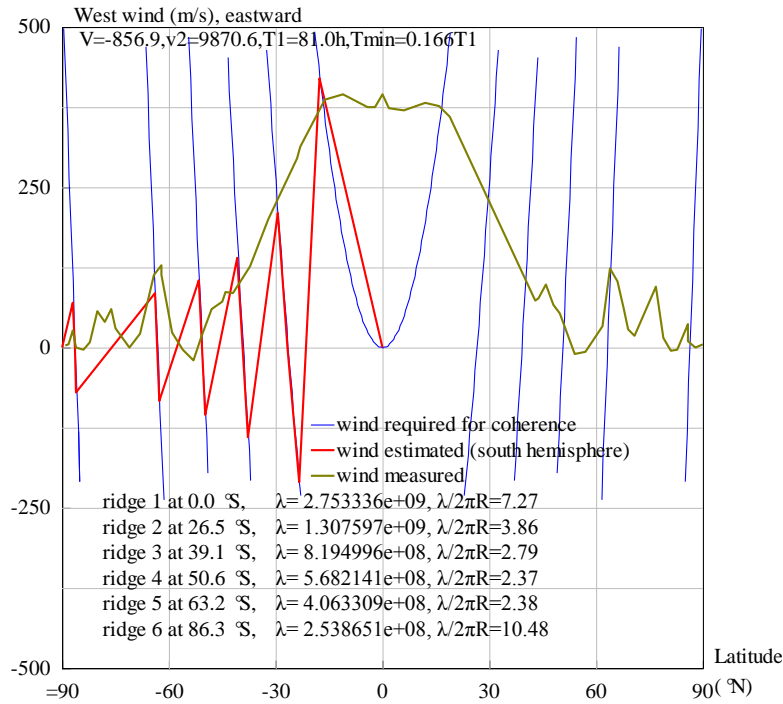


Figure 14 Calculation of zonal winds in the south hemisphere of Saturn.

<Clet2020 Script>// Saturn C source code [8]

```

double beta,H,M,r,rs, omega,v1,v2,V,V1,V2,T,T1,T2,a,b,c,d,w,Fmax,N[500],S[500],F[100],D[20];
int i, j, k, X, Y, m, n, s, f;
int
ZonalWind[118]={-89,2,-88,4,-87,26,-86,0,-84,-4,-82,8,-80,56,-78,40,-76,60,-75,30,-71,-1,-68,21,-64,113,-62,128,-62,113,-59,23
,-56,-4,-53,-20,-51,14,-48,60,-45,71,-44,86,-42,84,-37,126,-32,200,-24,294,-23,313,-16,386,-11,394,-4,375,-2,375,0,394,2,373,6,
369,12,381,16,376,19,360,43,73,44,76,46,98,48,66,50,53,54,-11,57,-7,59,8,62,33,64,123,66,102,68,60,69,27,71,18,77,95,79,14,8
1,-5,83,-4,86,36,86,10,88,-1,90,5,};
int main(){beta=7.175115e+13; H=SPEEDC*SPEEDC*SPEEDC/beta;
M=95.16*5.97237e24; rs=9.449*6.378e6; omega=2*PI/(10.6562*3600); T1=81*3600;
v2=rs*omega; Fmax=420; a=v2*v2-4*PI*H/T1; V=sqrt(a)-v2; T2=4*PI*H/v2*v2; T2=T2/T1;
V1=500; V2=-V1; SetAxis(X_AXIS,-90,-90,90,"Latitude#(°N)");V=-90;-60;-30;0;30;60;90;);
SetAxis(Y_AXIS,V2,V2,V1,"West wind (m/s), eastward;-500;-250;0;250;500;");
DrawFrame(0x0168,2,0xfffff); TextHang(-85,480,0,"V=%1f,v2=%1f,T1=%1fh,Tmin=%3fT1",V, v2,T1/3600,T2);
SetPen(1,0xff); f=0; m=0; V2=-V1/2; X=-20;Y=-120;
for(j=1;j<10;j+=1) { T=T1/j; Wind(); Polyline(n,N); Polyline(s,S); }
Polyline(2,S,X,Y,"wind required for coherence");Y=40;
SetPen(2,0xffff00);F[f+f]=90;F[f+f+1]=0;f+=1;Polyline(f,F);
Polyline(2,F,X,Y,"wind estimated (south hemisphere)");Y=40;
SetPen(2,0xafaf00); Polyline(59,ZonalWind); Polyline(2,F,X,Y,"wind measured");X=-80;Y=40;
for(i=0;i<m;i+=1) {a=D[i+i];TextHang(X,Y,0," ridge %d at %1f°S",i+1,a);//Y=-15;
a=a*PI/180;v1=(v2+D[i+i])/2; b= v1*T1/(i+1); c=b/(2*PI*rs*cos(a));
TextHang(X+50,Y,0,"λ= %e, λ/2πR=%2f",b,c);Y=40;}}
Wind(){n=0; s=0; c=PI/360; v2=omega*rs; a=v2*v2-4*PI*H/T; d=sqrt(a);
for(i=0;i<180;i+=1) { a=i*c; w=d-omega*rs*cos(a)-V*cos(a);
if(w>V2 && w<V1) {N[n+n]=i/2; N[n+n+1]=w; n+=1;}}
for(i=0;i<180;i+=1) { a=-i*c; w=d-omega*rs*cos(a)-V*cos(a);
if(w>V2 && w<V1) {S[s+s]=i/2; S[s+s+1]=w; s+=1;}}
//-----
if(n==0) return; c=180/PI;
w=-Fmax/j;a=(d-w)/(v2+V); b=-acos(a)*c; if(j==1) {b=0;w=0;} F[f+f]=b;F[f+f+1]=w; f+=1;
w=0;a=(d-w)/(v2+V); b=-acos(a)*c; if(j==1) {b=0;w=0;} F[f+f]=b;F[f+f+1]=w; D[m+m]=b; D[m+m+1]=d; m+=1; f+=1;
w=Fmax/j;a=(d-w)/(v2+V); b=-acos(a)*c; F[f+f]=b;F[f+f+1]=w; f+=1;
}#v07=?>A

```

10. Conclusions

In recent years, de Broglie matter wave has been generalized in terms of the ultimate acceleration on planetary-scale. This paper shows that the Jupiter's size and Saturn's size are the consequence of the interference of the generalized matter waves on planetary-scale. In this calculation, Jupiter's radius is determined as $7.1491e+7m$ with a relative error of 5.05%; Saturn's radius is determined as $5.80057e+7m$ with a relative error of 3.75%. This calculation also correctly predicts the locations of Halo ring and main ring for the Jupiter; ring A, B, C and D for the Saturn. In this calculation to the Earth, the tide near the equator has one maximal peak and 45 billows on the circumference around the Earth; the tide occurs every 24.91 hours, the width of the maximal peak of the tide is 1741km which lasts about 1.04 hours. At the latitude $35.4^{\circ}N$, its tide has two maximal peaks and 68 billows on its circumference around the Earth at the latitude, where the tide occurs every 12.45 hours. The equatorial belt has an eastward sea-flow at the speed of about 1m/s; on the north hemisphere, between latitudes $0.1^{\circ}N$ and $35.4^{\circ}N$ there is a larger ocean circulation; between latitudes $35.4^{\circ}N$ and $90^{\circ}N$ there is another ocean circulation. This paper shows that the Jupiter's south hemisphere contains five belts/zones that are separated by five coherent ridges at $0^{\circ}S$, $28^{\circ}S$, $41.6^{\circ}S$, $54.5^{\circ}S$ and $70^{\circ}S$, respectively, with the maximal wind of 120m/s, the Great Red Spot lives constantly at $23^{\circ}S$. the Saturn's south hemisphere contains six belts/zones that are separated by six coherent ridges, with the maximal wind of 420m/s. These predictions agree well with the experimental observations.

References

- [1]Huaiyang Cui, Determination of Solar Radius and Earth's Radius by Relativistic Matter Wave, Journal of Applied Mathematics and Physics, (2023)11:1, DOI: 10.4236/jamp.2023.111006.
- [2]C. Marletto, and V. Vedral, Gravitationally Induced Entanglement between Two Massive Particles is Sufficient Evidence of Quantum Effects in Gravity, Phys. Rev. Lett., 119, 240402 (2017)
- [3]T. Guerreiro, Quantum effects in gravity waves, Classical and Quantum Gravity, 37 (2020) 155001 (13pp).
- [4]S. Carlip, D. Chiou, W. Ni, R. Woodard, Quantum Gravity: A Brief History of Ideas and Some Prospects, International Journal of Modern Physics D, V.24,14,2015,1530028. DOI:10.1142/S0218271815300281.
- [5]de Broglie, L., CRAS,175(1922):811-813, translated in 2012 by H. C. Shen in Selected works of de Broglie.
- [6]de Broglie, Waves and quanta, Nature, 112, 2815(1923): 540.
- [7]de Broglie, Recherches sur la th orie des Quanta, translated in 2004 by A. F. Kracklauer as De Broglie, Louis, On the Theory of Quanta. 1925.
- [8]Clet Lab, Clet: a C compiler, download at <https://drive.google.com/file/d/1OjKqANcgZ-9V56rgcoMtOu9w4rP49sgN/view?usp=sharing>
- [9]Orbital Debris Program Office, HISTORY OF ON-ORBIT SATELLITE FRAGMENTATIONS, National Aeronautics and Space Administration, 2018, 15 th Edition.
- [10]Orbital Debris Program Office, Chinese Anti-satellite Test Creates Most Severe Orbital Debris Cloud in History, Orbital Debris Quarterly News, 2007, April,v11i2,
- [11]D. Wright, Space debris, Physics today,2007,10,35-40.
- [12]TANG Zhimei, DING Zonghua, DAI Liandong, WU Jian, XU Zhengwen, "The Statistics Analysis of Space Debris in Beam Parking Model in 78   North Latitude Regions," Space Debris Research, 2017, 17,3, 1-7.
- [13]TANG Zhimei DING, Zonghua, YANG Song, DAI Liandong, XU Zhengwen, WU Jian The statistics analysis Of space debris in beam parking model based On the Arctic 500 MHz incoherent scattering radar, CHINESE JOURNAL OF RADIO SCIENCE, 2018, 25,5, 537-542
- [14]TANG Zhimei , DING, Zonghua , DAI Liandong , WU Jian , XU Zhengwen, Comparative analysis of space debris gaze detection based on the two incoherent scattering radars located at 69N and 78N, Chin . J . Space Sci, 2018 38,1, 73-78. DOI:10.11728/cjss2018.01.073
- [15]DING Zong-hua, YANG Song, JIANG hai, DAI Lian-dong, TANG Zhi-mei, XU Zheng-wen, WU Jian, The Data Analysis of the Space Debris Observation by the Qujing Incoherent Scatter Radar, Space Debris Research, 2018, 18,1, 12-19.
- [16]YANG Song, DING Zonghua, Xu Zhengwe, WU Jian, Statistical analysis on the space posture, distribution, and scattering characteristic of debris by incoherent scattering radar in Qujing, Chinese Journal of Radio science, 2018 33,6 648-654, DOI:10.13443/j.cjors.2017112301
- [17]Huaiyang Cui, Relativistic Matter Wave and Quantum Computer, Amazon Kindle ebook, 2021.
- [18]Heng Li, Tides, Science Press, (1973) No13031.130, Beijing.
- [19]I. Morison, Introduction to Astronomy and Cosmology, John Wiley and Sons, Ltd., 2008.
- [20]Yohai Kaspi,et al, Comparison of the Deep Atmospheric Dynamics of Jupiter and Saturn in Light of the Juno and Cassini Gravity Measurements, Space Sci Rev, (2020),216:84, <https://doi.org/10.1007/s11214-020-00705-7>
- [21]Joshua Tollefsona,et al, Changes in Jupiter's Zonal Wind Profile preceding and during the Juno mission, Icarus, 296 (2017),163-178.
- [22]T.J.Dunkerton, Nearly identical cycles of the quasi-biennial oscillation in the equatorial lower stratosphere, Journal of Geophysical Research: Atmosphere, 122,8467-8493,(2017). Doi: 10.1002/2017JD026542
- [23]E.Garcia-Melendo,et al, Saturn's zonal wind profile in 2004-2009 from Cassini ISS images and its long-term variability, Icarus, 215(2011),62-74.